

Threshold photodetachment of H^-

K. R. Lykke,* K. K. Murray,[†] and W. C. Lineberger

*Joint Institute for Laboratory Astrophysics, National Institute of Standards and Technology
and University of Colorado, Boulder, Colorado 80309-0440
and Department of Chemistry and Biochemistry, University of Colorado, Boulder, Colorado 80309-0215
(Received 6 August 1990; revised manuscript received 21 February 1991)*

The electron affinities of atomic hydrogen and deuterium have been determined by tunable-laser threshold-photodetachment spectroscopy: the electron affinities of H ($F=0$) and D ($F=\frac{1}{2}$) are 6082.99 ± 0.15 and 6086.2 ± 0.6 cm^{-1} , respectively. The value for H is a 20-fold improvement over previous experimental determinations.

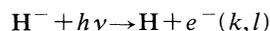
INTRODUCTION

The ion H^- is unique among negative ions in that its photodetachment spectrum was observed in space before it was observed in the laboratory. The continuous absorption of H^- was proposed by Wildt¹ in 1939 to be the main source of solar opacity in the region between 0.6 and 1.6 μm . Later comparisons between theory and solar observations confirmed this hypothesis.² In 1953, the hydrogen negative ion became the first negative ion to be studied by photodetachment in an ion beam.³ The electron affinity (EA) of the hydrogen atom has been determined experimentally by a variety of methods. Feldmann⁴ employed a 3-keV H^- beam crossed by the output of a laser-pumped optical parametric oscillator to determine the photodetachment threshold, obtaining an EA of 6081 ± 16 cm^{-1} . McCulloh and Walker⁵ determined the threshold wavelength for ion-pair formation in H_2 , using this energy to obtain the EA of the hydrogen atom via a thermochemical cycle. The ion-pair threshold was combined with the ionization potential of the hydrogen atom and the bond dissociation energy of H_2 to obtain a lower bound to the EA of 6081 ± 16 cm^{-1} . Chupka, Dehmer, and Jivry⁶ determined this same threshold energy to somewhat greater accuracy, obtaining a value of $6083 (+11, -3)$ cm^{-1} . Scherk⁷ derived an EA of 6085.5 ± 3.3 cm^{-1} from an analysis of H^- decay rates in the weak electric field of a particle accelerator.

The hydrogen atom is the only atom whose electron affinity is better known from *ab initio* calculations than from experiment.⁸ The two-electron H^- ion has invited elaborate *ab initio* calculations of both its nonrelativistic and relativistic energy. Pekeris⁹ has performed extensive Hylleraas-type variational calculations on H^- and has obtained a value¹⁰ of 6083.04 cm^{-1} with a reported accuracy of ≤ 0.01 cm^{-1} for the EA of the hydrogen atom. Aashamar¹¹ has also calculated the EA of H (including relativistic corrections) using Hylleraas-Scherr-Knight variational perturbation wave functions, obtaining a value 0.05 cm^{-1} higher than Pekeris. Even at the nonrelativistic level, the two results differ by 0.06 cm^{-1} . The reasons for the discrepancy are not obvious at present. Clearly it would be valuable to measure the EA of hydro-

gen to greater accuracy in order to provide a better experimental test of the quantum-mechanical results.

One of the most direct methods for measuring the EA of an atomic species uses a tunable light source to photodetach an electron from the negative ion. The cross section for the process



is obtained as a function of photon energy, where k and l are, respectively, the linear and angular momenta of the detached electron. For a small energy region above threshold, Wigner has shown¹² the energy dependence of the cross section to be

$$\sigma \propto k^{2l+1} \quad \text{or} \quad \sigma \propto \Delta E^{l+1/2},$$

where ΔE is the energy above threshold and l is the orbital angular momentum of the escaping electron. As an s electron is removed in H^- photodetachment, the outgoing electron has $l=1$ (p -wave threshold). The cross section rises with a $\Delta E^{3/2}$ dependence and has zero slope at threshold. This very small cross section near threshold makes precise measurements of the photodetachment threshold energy particularly difficult. Moreover, the difficulties are compounded by the presence of the hydrogen hyperfine structure, giving rise to two photodetachment thresholds within 0.05 cm^{-1} .

In this paper, we report high resolution (0.03 cm^{-1}) threshold photodetachment measurements for H^- and D^- ions. While individual hyperfine structure thresholds are not resolved, the cross-section data are fit to obtain electron affinities of H and D to accuracies of 0.15 and 0.6 cm^{-1} , respectively.

EXPERIMENTAL APPARATUS

The coaxial laser-ion beam photodetachment apparatus used in this study has been described in detail previously,¹³ and will only be briefly outlined. Hydride ions are produced by dissociative attachment of electrons to NH_3 in a hot cathode discharge. The ions are extracted, accelerated to between 2 and 3 keV, and mass selected. The H^- ions are merged with the output of a tunable laser along a 30-cm coaxial interaction region. The

≈ 2.5 -keV ion-beam energy provides a Doppler shift of approximately $+14 \text{ cm}^{-1}$ when the ion and laser beams are counterpropagated ($\uparrow\downarrow$) through the interaction region and -14 cm^{-1} when copropagated ($\uparrow\uparrow$). As discussed in the following section, both modes of operation and two ion-beam energies (2700 and 2160 eV) are employed to reduce several possible systematic errors. The products of photodetachment (both electrons and neutrals) are detected and counted as a function of photon energy.

The laser used in this experiment is a specially constructed F -center laser, shown schematically in Fig. 1. The laser uses an $(F_2^+)_A$ NaCl:OH $^-$ crystal, developed by Pollock and co-workers,¹⁴ that is pumped by 5 W from a cw 1.06- μm Nd $^{3+}$:YAG (yttrium aluminum gar-

net) laser. The filtered 365-nm light from a 100-W Hg lamp provides an auxiliary light that keeps the F_2^+ centers active. The laser can be configured as a standing-wave cavity with a linewidth of 1 GHz, a maximum output power of 500 mW, and a tuning range of 1.45 to 1.75 μm . It can also be configured as a single-frequency ring laser with an output power of 200 mW. The wavelength of the laser light is measured using a traveling Michelson interferometer λ meter¹⁵ using a polarization stabilized He-Ne laser as a reference. In addition, the 1.6- μm methane $2\nu_3$ absorption¹⁶ was measured simultaneously with the threshold detachment, enabling the accurate determination of the laser frequency to within 0.01 cm^{-1} .

Two problems exist that hamper the effort to obtain the EA of the hydrogen atom to high precision. The first is the magnitude and functional behavior of the cross section itself. Since the functional form of the threshold cross section is $\Delta E^{3/2}$, the cross section is zero at threshold and rises slowly above threshold. Absolute cross-section calculations^{8,17} indicate that the photodetachment cross section 1 cm^{-1} above threshold is only 10^{-21} cm^2 . The second problem is that the $F=1 \leftarrow F=0$ hyperfine splitting in the hydrogen atom of 0.047 cm^{-1} gives rise to a second photodetachment channel coupling very near the desired threshold. At the energy of the $F=1$ channel opening, the cross section for the $F=0$ channel (which has been open for 0.047 cm^{-1}) is only 10^{-23} cm^2 . This extremely small cross section rendered the very high resolution, single-mode laser, near-threshold data of little value in determining an accurate threshold energy. As a consequence, all of the data reported here were obtained with the standing-wave cavity configuration and a laser linewidth of 1 GHz. Approximately ten independent-threshold cross-section data sets were obtained for the H^- ion; a more limited set of photodetachment data was obtained for the D^- ion.

ANALYSIS AND DISCUSSION

Figure 2 shows the H^- photodetachment cross section over a 100-cm^{-1} region (1-GHz laser linewidth) near threshold, obtained with counterpropagating ion and laser beams. The solid line is a fit to the Wigner threshold law. The data were least-squares fit to the following equation:

$$\sigma(E) = A + B \{ (E - E_t)^{3/2} U(E - E_t) + W [E - (E_t + S)]^{3/2} U(E - (E_t + S)) \},$$

where $\sigma(E)$ is the relative photodetachment cross section, E_t is the threshold energy, E is the photon energy in cm^{-1} , W is the relative strength of the photodetachment cross sections to the two hyperfine levels in H, S is the hyperfine splitting (0.047 cm^{-1} in H, 0.011 cm^{-1} in D), A is a background offset, and B is a normalization constant. The Heaviside step functions $U(E)$ serve to cut off the threshold forms below each threshold. The data follows the $\Delta E^{3/2}$ threshold law to at least 60 cm^{-1} above the photodetachment threshold. The apparent threshold occurs at approximately 6069 cm^{-1} , redshifted approxi-

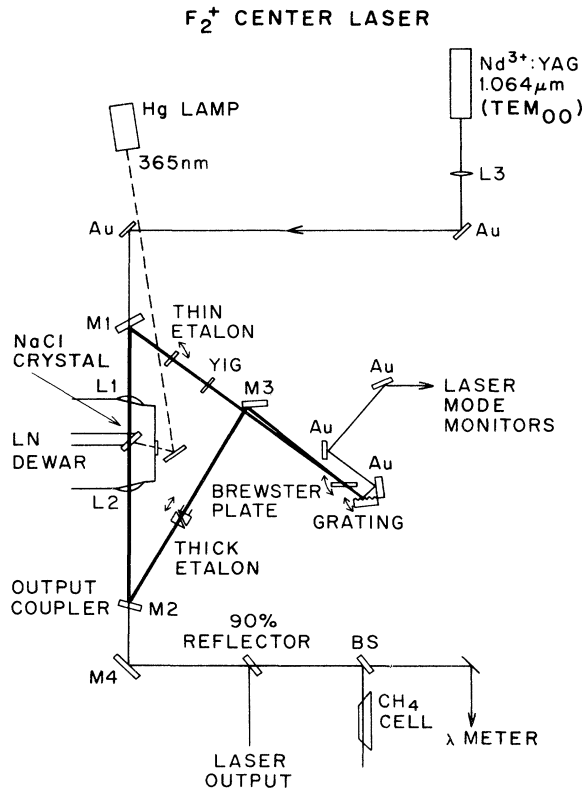


FIG. 1. Schematic diagram of the F -center laser. The active NaCl:OH $^-$ crystal is pumped by the Nd:YAG laser and the F centers are continually subjected to near-uv ionizing radiation from the Hg lamp. Other major elements include the following: M mirrors; Au, gold mirrors; L , lenses; BS, beam splitters; YIG, yttrium-iron garnet optical diode; LN, liquid nitrogen. The heavy line indicates the laser optical cavity when operated in the single-frequency ring configuration. In the broadband (1-GHz linewidth) setup, the mirror $M3$, étalons, and the YIG and Brewster plates are removed; the mirror $M2$ is rotated to form a standing-wave cavity with the grating and $M2$ as end mirrors and $M1$ as a folding mirror. The mirror $M4$ reflects the tunable-laser radiation, while eliminating residual 1.06- μm pump radiation.

mately 14 cm^{-1} due to the Doppler effect for counterpropagating photons and 2.7-keV H^- ions. The upper trace in the figure shows a portion of the R branch in the methane $2\nu_3$ overtone absorption spectrum, obtained simultaneously as a frequency calibration standard. A solid-line fit to the $\Delta E^{3/2}$ threshold law almost totally obscures the experimental data. The quality of the fit is very insensitive to changes of 0.25 cm^{-1} in the threshold energy, and an accurate threshold determination must utilize a more narrow energy range. Figure 3 gives examples of two sets of 1-GHz resolution photodetachment data taken over the more narrow energy range actually analyzed to obtain accurate threshold energies. One set was obtained with the laser propagating antiparallel ($\uparrow\downarrow$) to the ion beam and the second with the laser parallel ($\uparrow\uparrow$) to the ion beam.

The true threshold energy, correct to first order in the Doppler effect, is given by

$$h\nu_{\text{thr}} = h\nu_0^{\uparrow\uparrow}(1-v/c) = h\nu_0^{\uparrow\downarrow}(1+v/c).$$

The first-order Doppler effect contributes approximately 14 cm^{-1} at the 2- to 3-keV beam energies used. The average of the apparent threshold energies $h\nu_0^{\uparrow\downarrow}$ and $h\nu_0^{\uparrow\uparrow}$ obtained in the two different directions gives the true threshold energy $h\nu_{\text{thr}}$ correct to first order in the Doppler effect. Since the velocity terms cancel, the uncertainty of the ion-beam energy does not contribute to

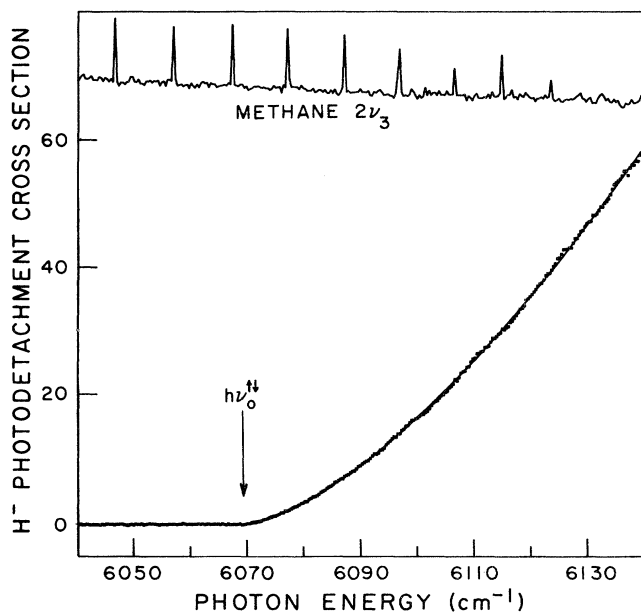


FIG. 2. A 100-cm^{-1} scan of the H^- photodetachment threshold cross section (arbitrary units) at 2.7-keV ion-beam energy. Dots represent the experimental results and the solid line is a fit to the Wigner ($\Delta E^{3/2}$) threshold law. The apparent threshold is redshifted approximately 14 cm^{-1} to 6069 cm^{-1} due to the antiparallel ($\uparrow\downarrow$) laser and ion beams. The simultaneously obtained methane absorption spectrum shown at the top of the figure is used as a frequency calibrant.

the uncertainty of $h\nu_{\text{thr}}$ to first order in the Doppler effect. The threshold, correct to both first- and second-order Doppler shifts, is given by

$$\begin{aligned} h\nu_{\text{thr}} &= h\nu_0^{\uparrow\uparrow} \frac{(1-v/c)}{[1-(v/c)^2]^{1/2}} \\ &= h\nu_0^{\uparrow\downarrow} \frac{(1+v/c)}{[1-(v/c)^2]^{1/2}}. \end{aligned}$$

The second-order Doppler effect adds approximately 0.02 cm^{-1} to the first-order threshold energy. The uncertainty in the ion-beam energy makes a negligible contribution to the second-order correction.

Several scans were obtained both parallel and antiparallel at two different beam energies. Since we want to obtain the threshold energy, two different beam energies were used to get a proper methane $2\nu_3$ transition near the corresponding threshold. The $R(5)$ line appears near $\nu_0^{\uparrow\downarrow}$

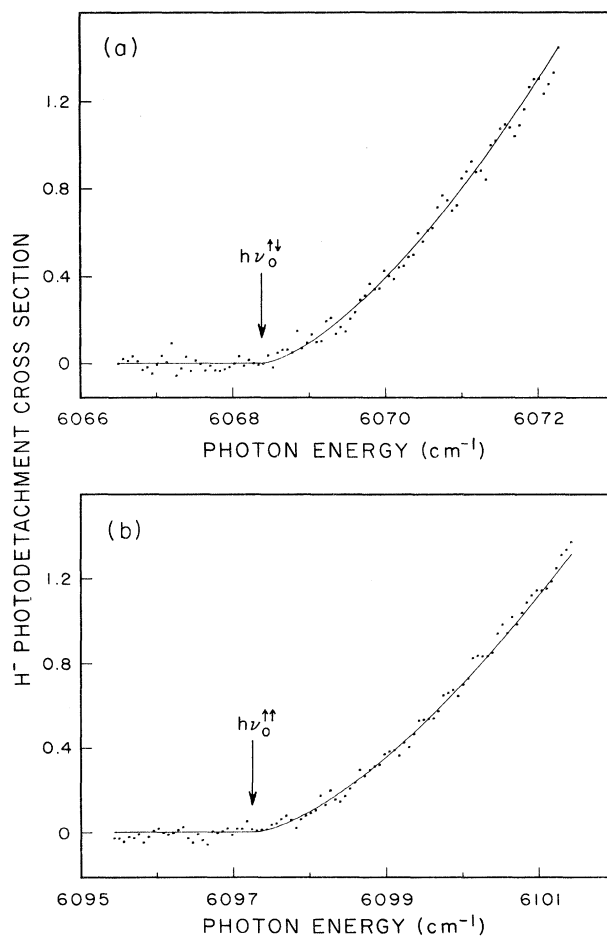


FIG. 3. Scans of the H^- ($F = \frac{1}{2}$) photodetachment threshold cross section (arbitrary units) at 2.7-keV beam energy with the laser and ion beams (a) antiparallel ($\uparrow\downarrow$) and (b) parallel ($\uparrow\uparrow$). In both cases, the dots represent the experimental results. The solid line is a fit to the data using a $\Delta E^{3/2}$ threshold law, and weighting transitions to the H ($F=0$) and H ($F=1$) thresholds by their 1:3 statistical weights.

for $E_b = 2700$ eV, and the $R(8)$ line appears near $\nu_0^{\uparrow\uparrow}$ at 2160 eV. The parallel and antiparallel data sets were separately analyzed to obtain $h\nu_0^{\uparrow\downarrow}$ and $h\nu_0^{\uparrow\uparrow}$. These two values were averaged to obtain $h\nu_{\text{thr}}$ to first order in the Doppler effect, and to this result was added the second-order correction to obtain the EA of ^1H ($F=0$) of 6082.99 ± 0.15 cm⁻¹. The EA was found to be insensitive to the $F=1$ to $F=0$ photodetachment channel weighting used in the fit: varying the strength of the $F=1$ channel from one to ten times the intensity of the $F=0$ channel did not change the EA obtained from the fit within the error limits quoted. The quoted results and fits use the expected 3:1 statistical weight.

A smaller number of scans of the $^2\text{H}^-$ (D^-) threshold region were undertaken and the data were fit to a similar threshold law to the one described in the preceding paragraph. In D , the $F=\frac{1}{2}$ and $\frac{3}{2}$ levels are separated by 0.011 cm⁻¹. Similarly, the EA of D ($F=\frac{1}{2}$) is determined¹⁸ to be 6086.2 ± 0.6 cm⁻¹. The difference in electron affinities of the two isotopes of 3.2 ± 0.7 cm⁻¹ is in good agreement with the predicted^{9,10} shift of 3.6 cm⁻¹.

The EA of 6082.99 ± 0.15 cm⁻¹ obtained in this work

agrees¹⁰ with both *ab initio* values of 6083.04 cm⁻¹ given by Pekeris⁹ and of 6083.09 cm⁻¹ by Aashamar,¹¹ but the experimental uncertainty is still a factor of 3 greater than the 0.05 -cm⁻¹ discrepancy between the *ab initio* values. In order to improve the accuracy of the experimental determination to the point that this disagreement could be tested, the threshold should be scanned with the single-frequency laser. The present version of the apparatus is not sensitive enough to perform this experiment, but plans are under way to incorporate a laser buildup cavity around the interaction region that will increase the available laser power by one to two orders of magnitude.

ACKNOWLEDGMENTS

The authors would like to thank Professor Cliff Pollock for his generous gifts of $\text{NaCl}:\text{OH}^-$ crystals and many valuable suggestions. We also thank Don Jennings for the loan of laser equipment. This work was supported by National Science Foundation Grant No. PHY 90-12244.

*Present address: Argonne National Laboratory, 9700 S. Cass Avenue, Argonne, IL 60439.

†Present address: Department of Chemistry, Rice University, Houston, TX 77251.

¹R. Wildt, *Astrophys. J.* **89**, 295 (1939).

²A. J. Deutsch, *Rev. Mod. Phys.* **20**, 388 (1948).

³L. M. Branscomb and W. L. Fite, *Phys. Rev.* **93**, 651A (1954); L. M. Branscomb and S. J. Smith, *ibid.* **98**, 1028 (1955).

⁴D. Feldmann, *Phys. Lett.* **53A**, 82 (1975).

⁵K. E. McCulloh and J. A. Walker, *Chem. Phys. Lett.* **25**, 439 (1974).

⁶W. A. Chupka, P. M. Dehmer, and W. T. Jivery, *J. Chem. Phys.* **63**, 3929 (1975).

⁷L. R. Scherk, *Can. J. Phys.* **57**, 558 (1979).

⁸H. Hotop and W. C. Lineberger, *J. Phys. Chem. Ref. Data* **14**, 731 (1985); **4**, 539 (1975).

⁹C. L. Pekeris, *Phys. Rev.* **112**, 1649 (1958); **126**, 1470 (1962).

¹⁰For comparison with experimental results, hyperfine-splitting corrections have been added to the *ab initio* values.

¹¹K. Aashamar, *Nucl. Instrum. Methods* **90**, 263 (1970).

¹²E. P. Wigner, *Phys. Rev.* **73**, 1002 (1948).

¹³U. Hefter, R. D. Mead, P. A. Schulz, and W. C. Lineberger, *Phys. Rev. A* **28**, 1429 (1983); R. D. Mead, K. R. Lykke, W. C. Lineberger, J. Marks, and J. I. Brauman, *J. Chem. Phys.* **81**, 4883 (1984).

¹⁴J. F. Pinto, E. Georgiou, and C. R. Pollock, *Opt. Lett.* **11**, 519 (1986); E. Georgiou, J. F. Pinto, and C. R. Pollock, *Phys. Rev. B* **35**, 7636 (1987).

¹⁵J. L. Hall and S. A. Lee, *Appl. Phys. Lett.* **29**, 367 (1976).

¹⁶D. H. Rank, D. P. Eastman, G. Skorinko, and T. A. Wiggins, *J. Mol. Spectrosc.* **5**, 78 (1960).

¹⁷H. P. Saha, *Phys. Rev. A* **38**, 4546 (1988), and references therein.

¹⁸The conversion factor from cm⁻¹ to eV is $1 \text{ eV} = 8065.5410(24) \text{ cm}^{-1}$, as given in E. R. Cohen and B. N. Taylor, *J. Phys. Chem. Ref. Data* **17**, 1795 (1988). The converted electron affinities are then 0.754195 ± 0.000019 eV for H and 0.754593 ± 0.000074 eV for D.